ENLO-SED: an innovative method for large-scale Strain Energy Density (SED) estimation in welded joints using structural stresses derived from Element Nodal LOads (ENLO)

Simone Lucertini, Giulia Morettini, Filippo Cianetti
University of Perugia, Department of Engineering, Via G. Duranti 93, 06125 Perugia, Italy
simone.lucertini@dottorandi.unipg.it, https://orcid.org/0009-0009-2822-6822
giulia.morettini@unipg.it, https://orcid.org/0000-0001-7313-135X
filippo.cianetti@unipg.it, https://orcid.org/0000-0002-1163-782X

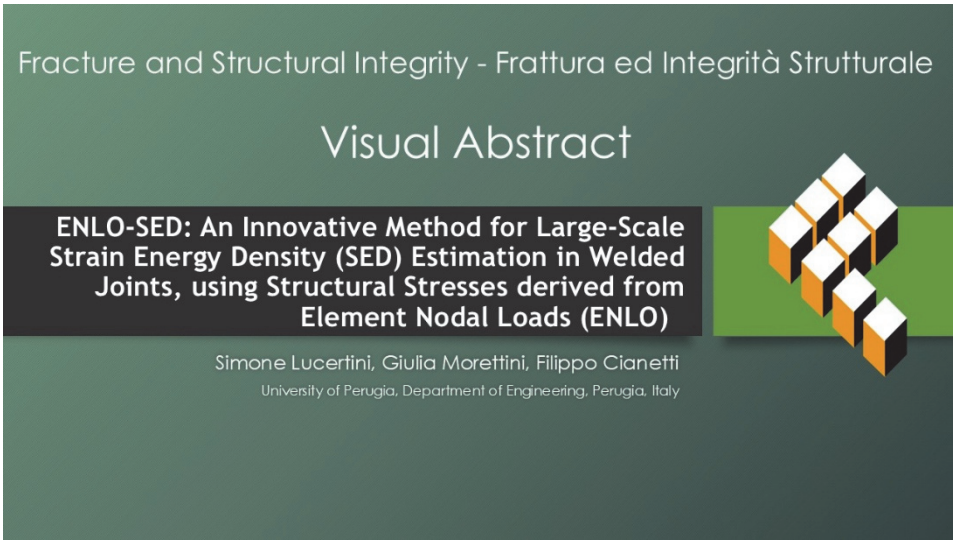

Citation: Lucertini, S., Morettini, G., Cianetti, F., ENLO-SED: an innovative method for large-scale Strain Energy Density (SED) estimation in welded joints using structural stresses derived from Element Nodal LOads (ENLO), Fracture and Structural Integrity, 74 (2025) 438-451.

Received: 28.07.2025
Accepted: 20.08.2025
Published: 22.09.2025
Issue: 10.2025

KEYWORDS. Welded joints fatigue, SED approach, Element Nodal LOads, Novel ENLO-SED method.

INTRODUCTION

Welded joints play a crucial role in mechanical industrial engineering, as they frequently represent critical connection points that directly influence the structural integrity and reliability of assemblies [1]. These joints are often the origin of structural failures, particularly under fatigue loading conditions. For these reasons, their assessment remains a major research priority in the academic world, aimed at improving the safety and durability of welded structures. Although significant progress has been made in the scientific field to enhance computational methods and fatigue analysis techniques [2], their effective application at the industrial level, particularly to large and highly complex welded structures, continues to present considerable challenges [3].On the other hand, the established techniques from the past,

which are still used today in welding design within the industrial sector, prove inadequate for current needs, necessitating the development and implementation of new methodologies.
The academic literature proposes different approaches for the fatigue analysis of welded joints that typically fall into two categories: the global design methods and the local approaches.
Global methods, such as the nominal stress approaches [4], are widely used, also in the industrial sector, due to their simplicity and the facility with which they can be applied to standard welded joints. However, these methods fail to account for local stress concentrations or defects in the joint, which can significantly influence fatigue behavior.
On the other hand, local methods, such as the Strain Energy Density (SED) approach [5-8], the Notch Stress Intensity Factor (NSIF) method [9], The Theory of Critical Distance [10,11], the Peak Stress Method [12,13] or The Critical Plane approach [14] offer more prospective by focusing on local quantities such as stress and strain. For most of these, their validity in terms of the results obtained is now widely recognized, as confirmed by numerous experimental and numerical comparison studies conducted over time by researchers [15-19]. However, these methods often require significant computational resources and specialized expertise. It thus becomes evident that their application is frequently limited to small-scale problems or simplified models, primarily due to the considerable computational time demanded during the pre-processing, solving, and post-processing stages. This limitation becomes particularly pronounced when addressing the practical challenges faced in the industrial sector.
The inherent complexity of real-world welded structures, characterized by different geometries, loading conditions, and defects, further complicates the application of these methods. The standard methodologies most commonly employed in the industrial field are, without doubt, the Nominal Stress Method, as referenced in Eurocode 3 and widely adopted across the European industrial applications, and the Hot-Spot Method illustrated in the British standard 7608. In addition to the methodologies above, the International Institute of Welding also reports the possibility of using the Notch Stress Approach (NSA) [20,21] and the Notch Stress Intensity Factor [22]. Among the approaches used in industry, we also find the Element Nodal LOad (ENLO) approach [23] and the Structural Stress Method [24]. The latter evolved into the Volvo Method, originally proposed by Volvo Car Corporation and Chalmers University of Technology and developed in cooperation with nCode software, particularly for automotive components welded. However, this structural stress-based approach is used with more general applicability on the ASME Boiler & Pressure Vessel Code VIII.
Although some of these methods have proven to be easy to implement (very often these methods are directly inserted as post-processing tools in finite element calculation codes) and computationally efficient, features that continue to make them attractive for industrial applications, they are increasingly considered obsolete from a scientific point of view. The academic research community has, as extensively discussed earlier, developed more advanced and accurate methodologies in recent years. Nonetheless, the industry's reluctance to abandon these consolidated approaches is largely due to the proven procedural simplicity in their application compared to the more sophisticated techniques proposed in scientific literature.
From this overview, it becomes clear that there is a pressing need to bridge the gap between these two worlds. The goal should be the development of a simplified yet robust methodology capable of combining the accuracy and reliability of academic models with the practicality and efficiency required in industrial contexts, thus empowering designers to adopt more effective fatigue assessment strategies in real-world welding applications.
To reach it, this paper introduces a novel technique: the ENLO-SED [25], which integrates the Strain Energy Density (SED) methodology with the use of structural stresses derived from the Element Nodal LOads (ENLO). The goal is to preserve the accuracy of the SED approach while reducing computational effort, making the method more suitable for large-scale industrial applications. The efficacy of ENLO-SED will be demonstrated through its application to a real welded joint case study and by comparing its performance with traditional SED methods in terms of accuracy, efficiency, and scalability. The method we propose can be effectively applied in industrial settings to quickly and reliably estimate the static and fatigue strength of complex joints in large-scale structures. It also helps pinpoint the most critical areas of a structure, where more detailed analyses, such as sub-modeling, or targeted physical testing can be carried out to ensure compliance with relevant standards.

THEORETICAL BACKGROUND

This section first presents the theoretical foundations and classical formulations of the two reference methodologies: the Strain Energy Density (SED) approach and the Element Nodal LOad (ENLO) method. Subsequently, the theoretical principles underlying the proposed combined methodology, developed by integrating key aspects of both approaches, are introduced.

Structural stresses from Element Nodal LOads method (ENLO)

This method is developed to assess stresses at critical locations of a welded structure, such as the weld toe or root, utilizing finite element analysis (FEA) results. In particular, the procedure uses the element nodal loads (forces and moments) of the mesh elements, here called ENLOs, to derive a mesh-insensitive stress value at the weld toe and root [24]. This value can subsequently be used for standard fatigue assessments.

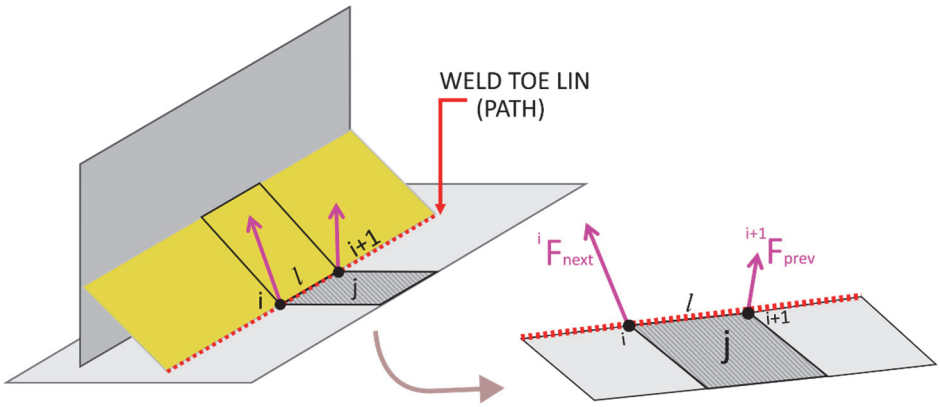

Figure 1: Illustrates a typical T weld joint modeled by shell elements, where the method was applied.

The element nodal loads "F" (three forces and three moments for a shell) are directly obtained for each element "j" at each node "i" for all the mesh elements representing the weld path.

There are several implementations of this approach; in the proposed one, a distributed load "$_{j}f$" is calculated at the mid-side of each mesh element "j", as evidenced by Eqn. 1, and transformed into an element-specific coordinate system, as illustrated in Fig. 2.

$$ {}_{j}f = \frac{\left[\frac{2}{l^2}\left(2\cdot {}^{i}F_{next} - {}^{i+1}F_{prev}\right) + \frac{2}{l^2}\left(2\cdot {}^{i+1}F_{prev} - {}^{i}F_{next}\right)\right]}{2} \tag{1} $$

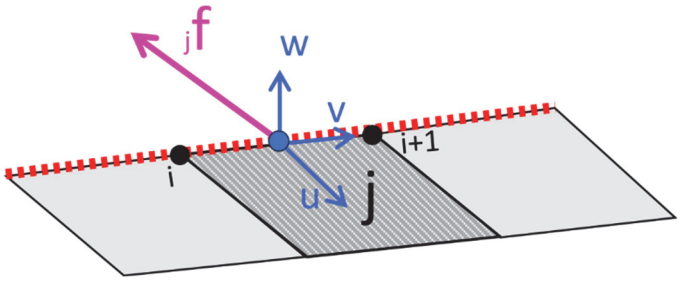

Figure 2: Detail of the derived load "f" on the element "j" and local coordinate system.

The stresses are then determined through straightforward considerations involving the element's cross-section, utilizing the associated Area and Moment of Inertia per unit length. The resulting so-called "structural stress" is finally expressed as a combination of the normal (membrane stress) and bending components, as expressed in Eqn. 2 and Eqn. 3 for the top and bottom surfaces.

$$ {}_{j}\sigma_{top} = {}_{j}\sigma_{N} + {}_{j}\sigma_{top,M} = \frac{{}_{j}f_{u}}{t} + 6\frac{{}_{j}m_{v}}{t^2} \tag{2} $$

$$ {}_{j}\sigma_{bottom} = {}_{j}\sigma_{N} - {}_{j}\sigma_{bottom,M} = \frac{{}_{j}f_{u}}{t} - 6\frac{{}_{j}m_{v}}{t^2} \tag{3} $$

Similarly, it is possible to calculate the shear stress along the weld toe through Eqn. 4 and Eqn. 5:

$$ {}_j\tau_{top} = {}_j\tau_{from\ f_v} + {}_j\tau_{from\ m_u} = \frac{{}_j f_v}{t} + 6\frac{{}_j m_u}{t^2} \tag{4} $$

$$ {}_j\tau_{bottom} = {}_j\tau_{from\ f_v} - {}_j\tau_{from\ m_u} = \frac{{}_j f_v}{t} - 6\frac{{}_j m_u}{t^2} \tag{5} $$

where "t" represents the plate thickness at the weld toe (weld toe mesh elements). This approach is referenced in [35].
These stresses can then be used to evaluate the joint's proof of strength through any static and fatigue stress-based calculation methods.
This technique presents significant advantages for large-scale industrial applications. Notably, its reliance on shell elements enables seamless implementation of complex geometries and assemblies, even those involving an extensive number of joints. Another key benefit is that the structural stress evaluation is purely a post-processing task, making it applicable to feeding the output of a prior static FEA. Additionally, this methodology does not require refining the mesh at the weld toe or root, so it involves a relatively small number of mesh elements and nodes, resulting in very low computational demand. For all these reasons, the approach has been incorporated into several commercial software tools, such as nCode DesignLife and Dassault Simulia FeSafe (even if using different formulations).
However, the method's simplifications result in a lower level of accuracy compared to more advanced techniques, and its use is limited to situations where no other methods are suitable. The main reason is that it relies on the stress on a notch, which is a quantity somehow difficult to perfectly correlate with the measured fatigue strength. The stress used in this method, for mode I fracture, is expressed in Eqn. 6 and represents the worst combination between the normal and bending stress (shell top layer).

$$ S_{ENLO} = \frac{{}_j f_u}{t} + 6\frac{{}_j m_v}{t^2} \tag{6} $$

The Strain Energy Density method (SED)

This approach employs a local method based on the strain energy density (SED) evaluated within a small volume centered on the geometrical notch [5]. For welded joints, this corresponds to a circular region centered at the weld toe with a radius R_0, as shown in Fig. 3:

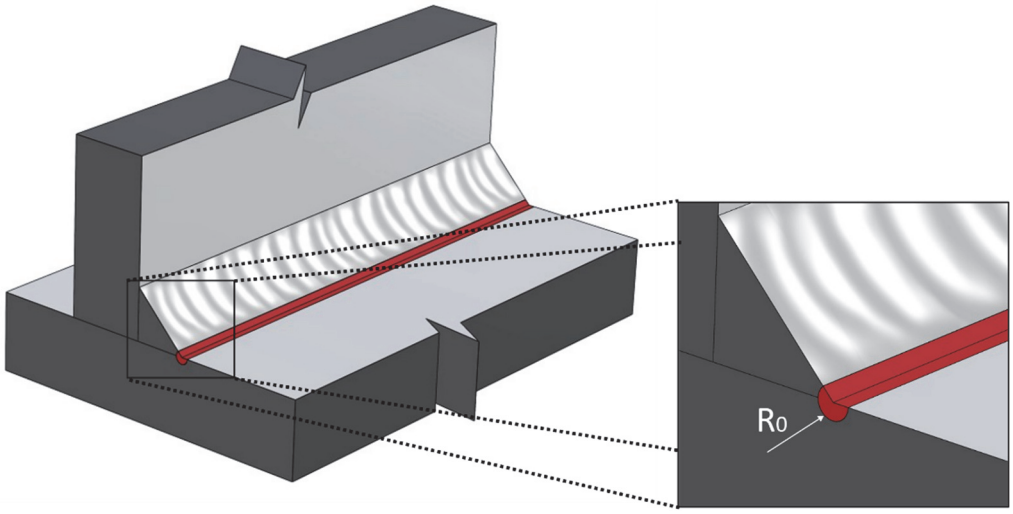

Figure 3: Details of the critical volume to retrieve the SED.

The case examined in this paper ($90°$ welded joint) is the typical application of SED method, where the nominal geometry is characterized by a $45°$ weld bead so consequently the angle between the plates and the weld is $\alpha = 135°$. The toe line, for the reference 3D model, is created with no smoothing radius [5, 15] This is one of the benefits of this method. The

characteristic critical radius R_0 is determined solely by the material properties; for structural steel, the most widely used value is $R_0 = 0.28\,mm$ [5,15].

The strain energy density $\bar{W}_{SED}$, generated by a specific load condition, evaluated within this critical volume can be accurately calculated through finite element simulations of solid structures.

This value can be compared to the critical threshold SED value, W_c which represents the fatigue limit for the strain energy density. It can be asserted that if $\bar{W}_{SED}$ remains below ΔW_c, there are no time-limitations on the application of the considered load as expressed in Eqn. 7.

$$\bar{W}_{SED} < W_c \tag{7}$$

This method can be implemented using finite element analysis (FEA). Results have demonstrated excellent accuracy when validated against numerous experimental tests. It is particularly effective for complex joint configurations and, as a local approach, it allows the evaluation of production defects such as misalignments in the plates. However, this method necessitates the definition of a "control volume" in the FEA model, which can be a time-intensive task for intricate structures or large-scale applications.

The SED calculation, in its standard formulation, relies on solid (brick) mesh elements or their 2D equivalents, making it incompatible with the shell elements representation. While the method itself is insensitive to mesh refinement, the small size of the control volume requires a significant number of elements even for simple joints, leading to substantial computational demands as well as notable effort to extract and process results. These factors make this technique well-suited for detailed investigations but less practical for large-scale industrial use.

The ENLO-SED method

This method is founded on the fact that the two above-mentioned methods can be compared using the ENLO-SED correlation [25]. It is possible to start by asserting that, as widely demonstrated in [7], the strain energy density (SED) at the weld toe primarily depends on the loads (forces and moments) applied to the section nearest to the toe, with minimal influence from distant loads. This implies that a full-scale finite element (FE) model can be replaced by a simplified shell model, allowing the local loads to be directly compared to the corresponding local SED.

The correlation between these methods can be carried out by using Eqn. 8, that is comparing similar quantities. The structural stresses (S_{ENLO}) derived from Eqn. 6 using the ENLOs are, through this new method, converted to an equivalent linear-elastic strain energy: the $\bar{W}_{ENLO\_SED}$.

$$\frac{S^2_{ENLO}}{2E} \cdot \xi_{(core,t)} = \bar{W}_{ENLO-SED} \tag{8}$$

The $\xi_{(core,t)}$ represents a "correlation parameter" that depends on the local geometry ("*core*") characteristics of the welded joint analyzed and on the thickness ("t") of the plate as shown in Fig. 4. The procedure by which this correlating parameter was obtained is described in greater detail in [7]. It is sufficient to remember that this parameter represents the multiplicative factor that fine-tunes the energy obtained via the Nodal Load method to fit the function of the energy derived from the classical SED. In this particular case, we use a simple L welding joint, illustrated in Fig. 4, as a calibration case to derive the expression of the correlation parameter illustrated in Eqn. 9, as a function of the thickness ("t").

This model was loaded with a distributed unitary moment at the right edge and all 6 DOFs locked on the top edge as shown in Fig. 4.

$$\xi_{(t)} = 0.632 \cdot e^{(0.193 \cdot t)} \tag{9}$$

Fig. 5 plots the best-fit function of the correlation parameter for the analyzed welding geometry ("core") by the plate thickness ("t").

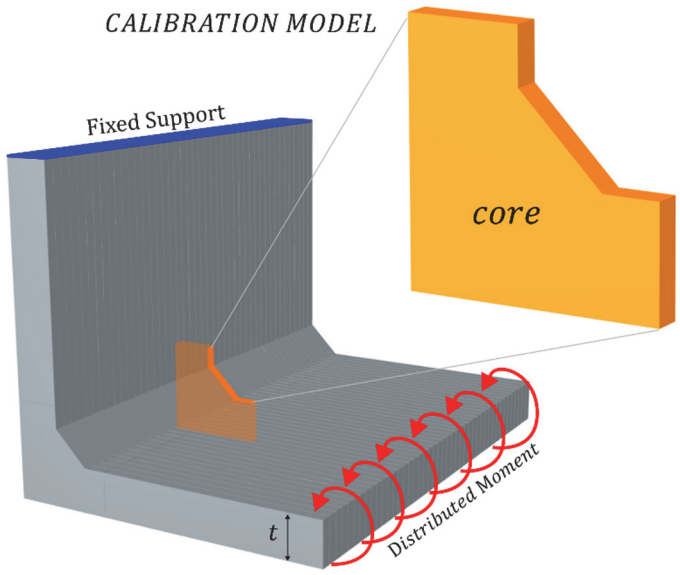

Figure 4: Calibration model, with the "core" highlighted, and the Boundary Conditions.

Fig. 5 shows that for a thickness range between 2.5 mm and 6.0 mm the normalized value of ξ stands between 1.0 and 2.0. The knowledge of the $\xi_{(core,t)}$ function enables the estimation of the Strain Energy Density (SED) from the element nodal loads. In the following paragraphs, we will demonstrate that the same equation, derived from a calibration case, can be extended to different geometries. Consequently, this will allow the ENLO-SED method to be applied to arbitrarily shaped geometries for SED estimation.

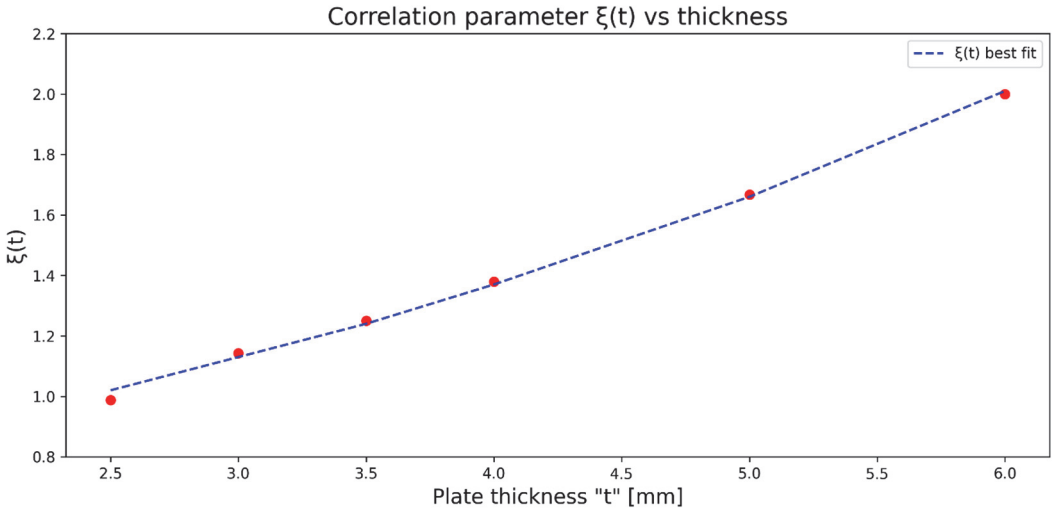

Figure 5: Correlation parameter ξ(t) for an "L" joint core, from the calibration model.

GLOBAL APPLICATION: THE CASE STUDY

As demonstrated in the previous paragraphs, ENLO-SED correlation allows us to estimate a complex quantity such as local SED, using only a simplified shell-based FE model. This is a leading advantage of this approach since it permits the SED method to be applicable to industrial complex models, with a huge quantity of welded joints, requiring a very small user intervention and a minimal computational effort.

In this paper, the ENLO-SED will be applied to a common joint consisting of a rectangular tube welded to a plate, as illustrated in Fig. 6. This application is widely used in any industrial sectors. Some structures might have dozens and even hundreds of these joints, with different geometrical parameters or suffering different loading conditions (static and dynamic).

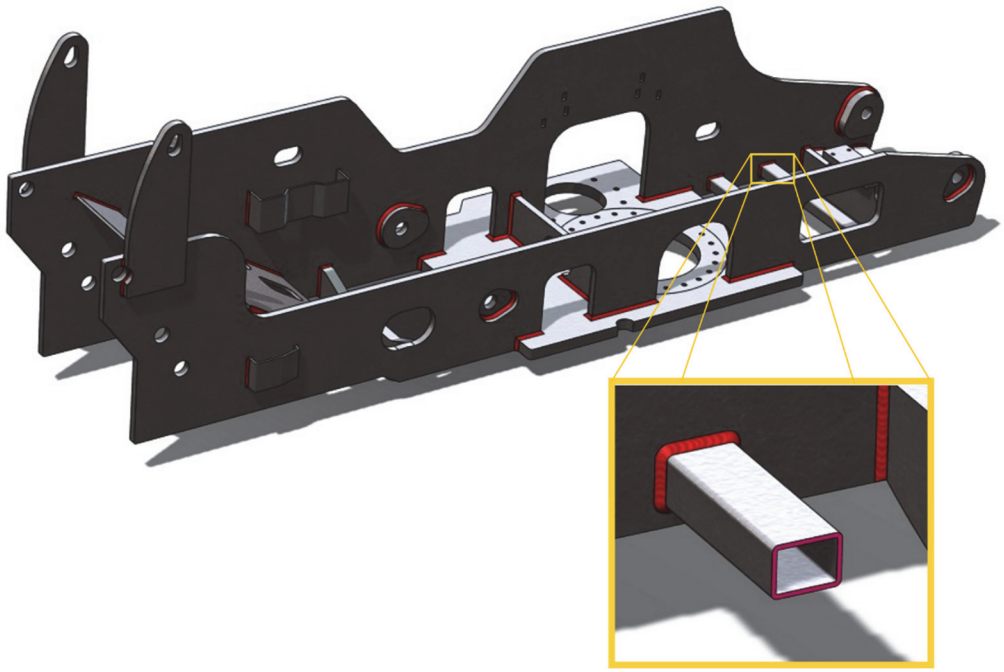

Figure 6: Example of a complex welded structure and detail of this analysis.

Since the ENLO-SED is a local method, it can be applied in pure post-processing to any joint independently, as evident from the workflow represented in Fig. 7.

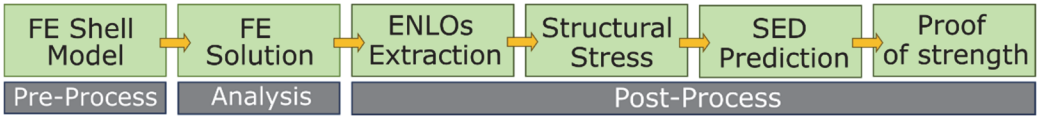

Figure 7: Operative workflow to apply ENLO-SED method.

In this very specific case, a Python 3 script was used to perform the calculation and the results extraction. In particular, since Ansys was used as a solver, the dedicated Ansys-DPF Core library was used to extract and process the results information. The workflow shows 3 main stages: Pre-processing, Analysis, and Post-Processing. In the first one, the FE model is prepared as a common shell model, including the representation of the weld bead for the joints that are to be investigated. Then the Loads and Boundary Conditions are applied, and the analysis is solved as usual. The strength calculation takes place in the Post Processing phase, from the FEA results. From these results, the Element Nodal loads (forces and moments) are retrieved for all the elements connected to the weld toe. The structural stresses are then calculated as shown in Eqn. 6. Finally, the Structural stress $\left(S_{ENLO}\right)$ is converted to the equivalent elastic SED through the correlation Eqn. 8 and the proof of strength (static or fatigue) is then executed as any SED-based by substituting the energy value obtained $(\Delta\bar{W}_{ENLO-SED})$ into Eqn. 7, thus, obtaining the Eqn. 10.

$$\Delta\bar{W}_{ENLO-SED} < \Delta W_c \tag{10}$$

The focus of this analysis is to demonstrate that the correlation parameter "$\xi_{(t,\,core)}$" depends only on the local loads (element-nodal loads) on the weld line path, so it is still valid if the global loads and boundary conditions change. In this application, referencing Fig. 8, the structure is constrained at the surface marked "A" locking all 6 DOFs of the mesh nodes, while a force of 1N is applied to the surface marked "B".

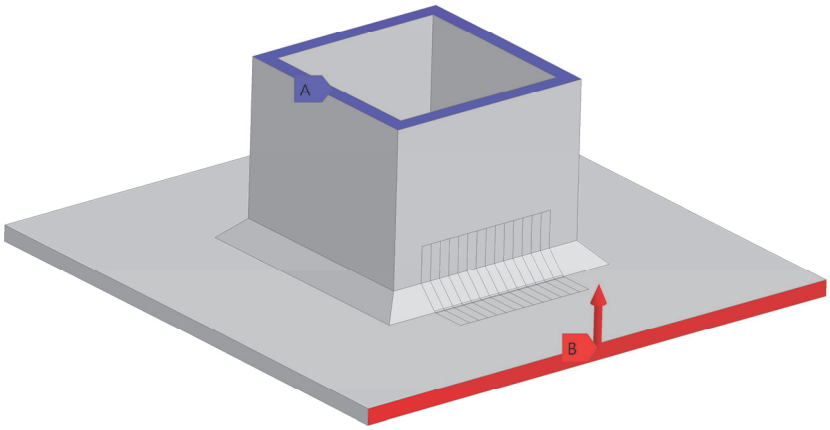

Figure 8: Boundary conditions. Marker A: Fixed DOFs, Marker B: External Load.

As previously shown in Section 2.3 in the calibration model, a distributed moment was applied to the far edge. It is clear that the boundary conditions are completely different between this application and the calibration one.
It should also be noted that, due to the formulation used for the structural stress from ENLOs, this application is valid for the Mode-I fracture, while the extension to Mode II and III will be left for future in-depth analysis. Full penetration weldments have been considered, so the crack initiation point is always located on the weld toe, which represents the most common situation in many industrial applications.
It is important to note that the results presented here are valid for plate thicknesses ranging from 2.5 mm to 6.0 mm and for a fully penetrated 45° weld bead. Future analyses will be conducted to explore a broader range of geometries.
Having clarified these fundamental aspects, the purpose of the following paragraphs is to analyze a full scale (solid) model of a single welded joint through the classical SED approach and compare the results obtained, both the numerical terms (Strain Energy Density quantity) and in terms of computational time, with the prediction based on ENLO-SED applicated to is simplified shell version.

MODELLING OF THE JOINT GEOMETRY

This section provides a detailed description of the joint geometry. To apply the two different approaches, the joint is represented in two distinct ways: a *full-scale model*, derived from the SED application using a detailed solid representation, and a *simplified model*, represented as a shell, which is suitable for the ENLO-SED application.

Reference full-scale solid model

This model has been created using detailed 3D geometry. In order to guide the mesh and to make the SED applicable along the entire weld line length, the bodies have been split into smaller chunks with shared topology (mesh continuity) as shown in Fig. 9. This operation requires user intervention and represents a first time-consuming task that must be repeated for each joint analyzed.
The mesh is composed of 20-nodes solid brick "high quality" elements and to grant the results convergence, the size of the elements is smaller in the SED critical area and slowly decreased on far zones, as visible in Fig. 10.
It is finally crucial to underline that this model is bound to a specific plate thickness (t), so in order to iterate over different values, it is necessary to change the geometry, hence re-mesh the entire model and, of course, re-launch the FE Analysis.
With these assumptions, the total number of elements (and so mesh nodes) is huge, even considering a single weld line of a unique joint. The mesh-element size has been optimized through a sensitivity analysis to grant the required convergence on the result values while avoiding the elements being excessively small.
As a reference, for the proposed model, with the optimized mesh quality on the red weld toe line shown in Fig. 10, the total number of elements is between 54441 and 68561, and the nodes are between 141682 and 160527, depending on the plate's thickness (from 3mm to 6mm).

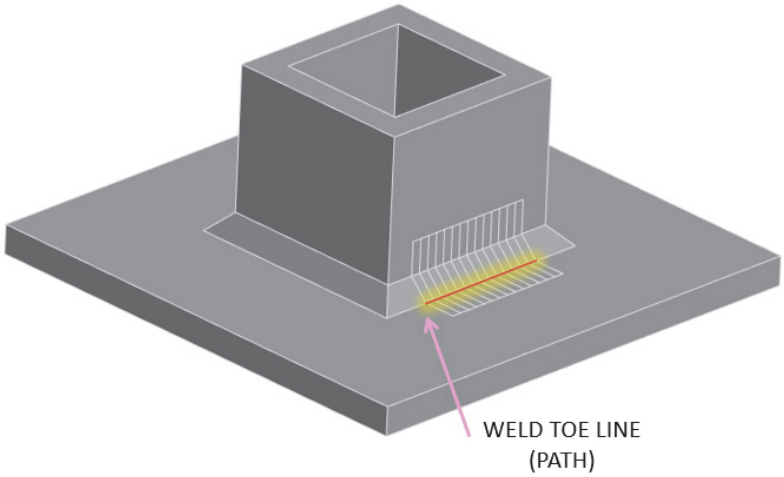

Figure 9: Solid model. Weld's toe is highlighted.

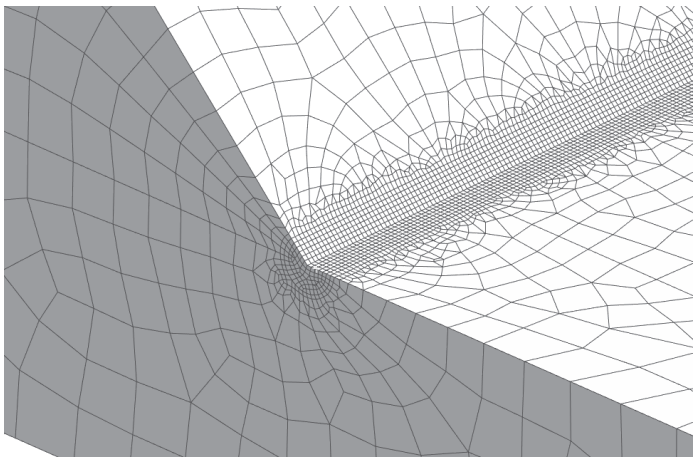

Figure 10: Details of solid mesh (hex20) around the critical volume at the weld toe.

Shell model

This second model, shown in Fig. 11, is derived from the 3D geometry and requires few pre-processing operations, such as extracting the center shell from the plates and for the weld bead. These operations are very common and almost any CAD has specific features for this application.

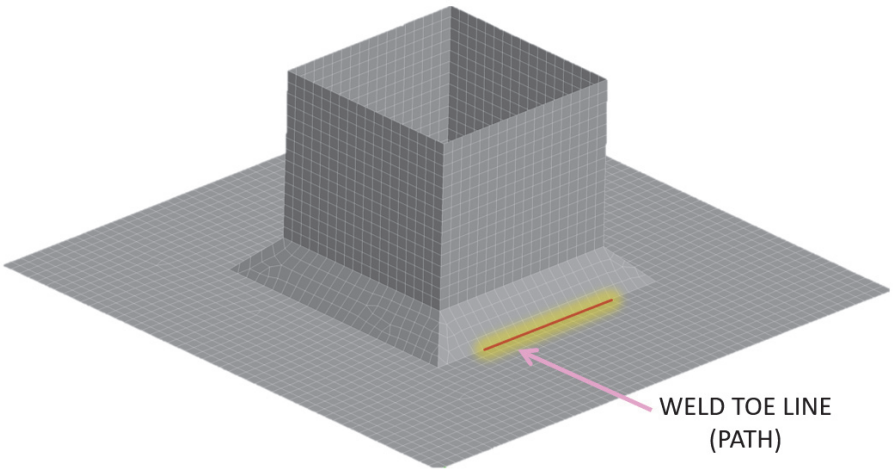

Figure 1: Simplified shell model. Weld's toe is highlighted.

The mesh, visible in Fig. 11, is realized using "linear" shell elements (4-nodes) among the weld line (3-nodes) triangles could be used as well, while parabolic side 8-nodes shells could be used for increased quality on curve geometries.
For this simplified geometry, the total number of elements is 4200, and the number of nodes is 4198.
As demonstrated in [1] and [2], extracting structural stresses from element nodal loads does not require an extra-fine mesh. Therefore, a mesh size of 2 mm was used in this study. However, larger mesh sizes could also be employed effectively to further reduce the total number of elements and nodes. It is also immediately noticeable that this model is extremely reduced in terms of complexity and computational requirements, and so adapted to be used with large and even huge geometries.
It is important to note that, assuming a small error, in this case, the CAD model can be unique among all the thicknesses, so there's no need to re-mesh the model, hence multiple values of t can be easily explored by parametrizing it, without any other user intervention.

RESULTS ANALYSIS AND COMPARISON

This section shows the results obtained with the ENLO-SED methodology and the comparisons in terms of computational time performance and accuracy of results obtained with the "standard" SED methodology.

Comparison of computational time performance.
As a preliminary consideration, it is possible to state that the shell model, useful for the ENLO-SED methodology, outperforms the 3D model, necessary for the SED method, in terms of preparation and *Pre-processing* time. The extraction of the mid-surface and the creation of the weld bead require, in fact, fewer operations and are computationally faster than the critical volume definition and weld path segmentation necessary in the 3D model.
This aspect is even more pronounced during the *Design stage*, where thickness modifications, in the solid model, require a geometric adaptation and a re-meshing phase, whereas using a shell model, it is possible to implement the thickness variation instantly by adjusting a single parameter.
However, the advantages previously described in the *Pre-Processing* and *Design* phases cannot be objectively quantified in terms of time, as they heavily depend on the operator's skills and expertise. Nevertheless, the benefits of using the simplified shell model in terms of computational efficiency can be further emphasized by examining the objective results presented in Tab. 1, which specifically pertain to the *Meshing* and *Solution phase* of the model.
As it is visible, in Tab. 1, the mesh advantages are clear both in terms of the number of nodes and elements necessary for the convergence of the solution and in terms of meshing times. The shell model contains only between 12.9% and 16.3% of the total number of elements compared to the solid model. This reduction significantly impacts both meshing and solution times.

	3D Model	Shell Model
Number of Mesh elements	54441 (t=3mm) 68561 (t=6mm)	4200 (all values of "t")
Number of Mesh nodes	141682 (t=3mm) 160527(t=6mm)	4198 (all values of "t")
Mesh time	33s	2s
Solution Time	15s	3s

Table 1: Performance comparison between the models.

Considering the systems analyzed, the *Meshing time* for the shell model, in fact, is less than 2 seconds, while for the solid one, it is around 33 seconds, as shown in Tab. 1, so 15 times slower. Similar behavior is seen through the *Solution time* where the shell model solves in 3 seconds and the solid one lasts in the mean of 15 seconds, so around 5 times slower.

Accuracy of results

The Strain Energy density on the control volume is retrieved from the 3D full-scale models, varying the plate thickness from 3.0mm to 6.0mm, and plotted in Fig. 12 as continuous lines as a function of the weld path. Due to the traverse deformations, the SED value is not constant along the weld line, resulting in a higher value around the corners and a lower value in the center.

The same analysis was done for the shell model, where the strain energy density value is estimated through the ENLO-SED methodology and represented in Fig. 12 through the dashed lines for all the thickness cases analyzed.

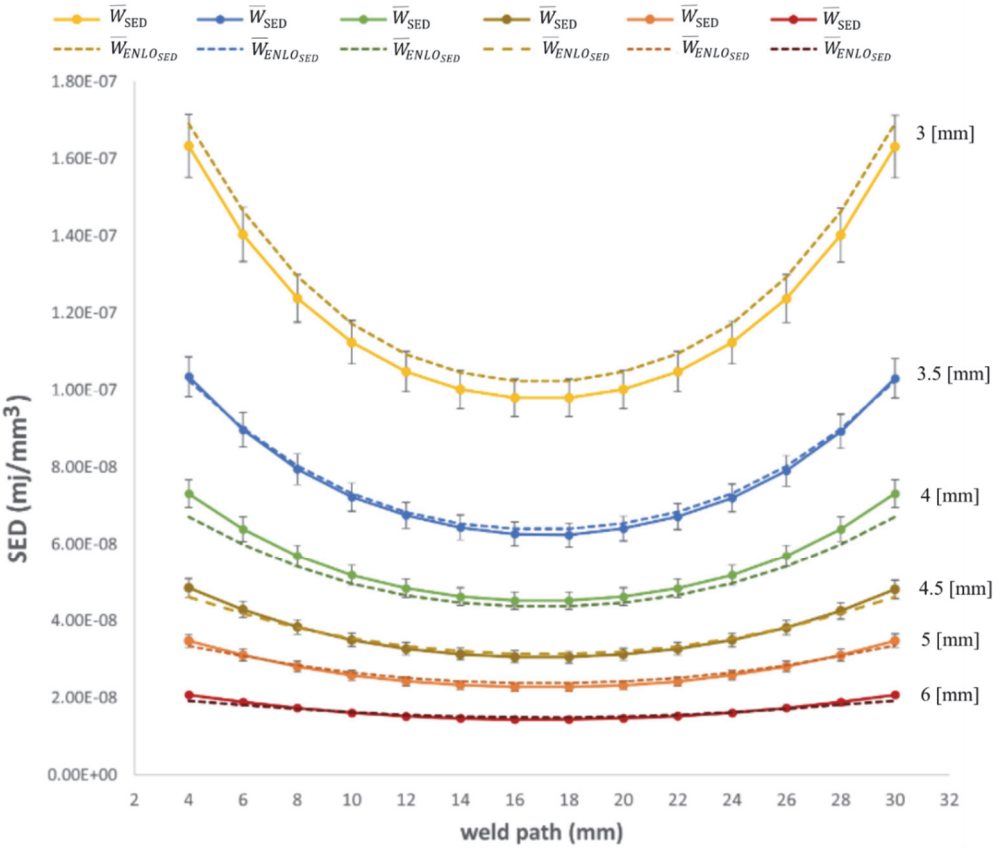

Figure 12: Comparison between the reference (W_{SED}) and the estimated value ($W_{ENLO\text{-}SED}$) for the Strain Energy Density at different values of "t". 5% error bars are shown for reference values.

It is immediately noticed, from Fig. 12, that the strain energy density estimated from ENLO-SED methodology follows the reference behavior evaluated by the original SED method along the weld line. Remembering that for the simplified analysis, the boundary conditions are completely different from the calibration model, this means that the correlation parameter ξ is still valid, depending only on the core geometry and the plate's thickness.

The absolute error between the reference and the estimation is globally lower than 8%, as shown in Fig. 13 and it is calculated by means of the following formula:

$$error\ \% = \left| \frac{W_{SED} - W_{ENLO-SED}}{W_{SED}} \right| \cdot 100 \tag{15}$$

Considering the time and hardware benefits of the simplified model stated previously, and the typical error levels of a finite element simulation, this means that the ENLO-SED methodology is capable of estimating the strain energy density on a weld line with high reliability and extremely low computational effort.

This result enables the extension of the analysis to large-scale models, where managing geometrical complexity and a high number of joints becomes increasingly challenging. In such cases, traditional approaches that rely on high-quality 3D meshing may be computationally prohibitive, requiring excessive resources and time. The simplified methodology

demonstrated here provides a feasible alternative, ensuring both efficiency and accuracy while maintaining the necessary level of detail. By leveraging this approach, it becomes possible to analyze complex structures that would otherwise be impractical to model using conventional 3D meshing techniques.

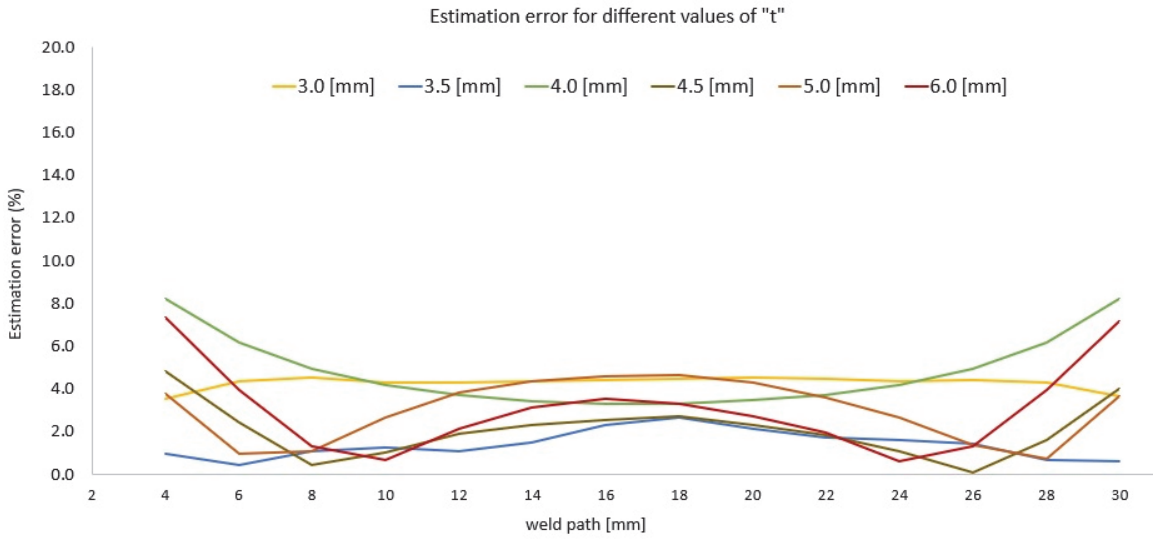

Figure 13: Absolute error analysis. Estimation vs reference.

Conclusions

This study has demonstrated the potential of applying the innovative ENLO-SED methodology for the prediction of the resistance of welded joints, applicable, thanks to its computational speed and accuracy, in multiple industrial sectors. In addition to its traditional use in basic contexts, in fact, the method can find a strong applicative response in the estimation of the strain energy density (SED) of welded joints (in conditions of mode I crack opening), even of high complexity. Using a simplified shell model, in fact, and adopting the same correlation parameters previously validated by the same Authors, we have achieved a high level of agreement with detailed 3D models, maintaining a prediction error within 8%. In addition to accuracy, the proposed method significantly improves computational efficiency, reducing meshing time by a factor of 15 and solution time by a factor of 5. These improvements enable the application of this methodology to large-scale industrial models with multiple welded joints, providing a practical solution for early-stage design assessments or integrity assessments with limited computational resources.

The results highlight the robustness and scalability of the method, paving the way for wider adoption in engineering workflows where time and resource constraints are critical. Future research will aim to extend this methodology to accommodate more complex geometries and include crack initiations under mode II and mode III loading conditions.

References

[1] Vatnalmath, M., Auradi, V., Bharath, V., Bharadwaj, A., Gowda, C. and Nagaral, M. (2025). Microstructure, mechanical and fractographic behaviour of the diffusion welded joints of AA2219 and Ti-6Al-4V for aerospace applications. Fracture and Structural Integrity, 19(71), pp. 37–48. DOI: https://doi.org/10.3221/IGF-ESIS.71.04

[2] Lufan, Z., Boshi, J., Pengqi, Z., Heng, Y., Xiangbo, X., Ruizhuo, L., Jingjing, T. and Caixia, R. (2023). Methods for fatigue-life estimation: A review of the current status and future trends. Nanotechnol. Precis. Eng., 6(2), 025001. DOI: https://doi.org/10.1063/10.0017255.

[3] Castro, D., Illade, J., Gonzalez, N., Pintos, S. and Russello, M. (2025). The Advanced Real-Time Monitoring of New Welding Processes in the Aircraft Industry. Engineering Proceedings, 90(1), 7. DOI: https://doi.org/10.3390/engproc2025090007

[4] Al Zamzami, I. and Susmel, L. (2017). On the accuracy of nominal, structural, and local stress based approaches in designing aluminium welded joints against fatigue. International Journal of Fatigue, 101, pp. 137–158.

DOI: https://doi.org/10.1016/j.ijfatigue.2016.11.002
[5] Foti, P., Crisafulli, D., Santonocito, D., Risitano, G. and Berto, F. (2022). Effect of misalignments and welding penetration on the fatigue strength of a common welded detail: SED method predictions and comparisons with codes. International Journal of Fatigue, 164. DOI: https://doi.org/10.1016/j.ijfatigue.2022.107135
[6] Meneghetti, G., Campagnolo, A. and Berto, F. (2019). Averaged strain energy density estimated rapidly from the nodal stresses by FEM for cracks under mixed mode loadings including the T-stress contribution. Fracture and Structural Integrity, 13(49), pp. 53–64. DOI: https://doi.org/10.3221/IGF-ESIS.49.06
[7] Chen, Z., Wang, P., Liu, Y. and Qian, H. (2025). Analysis of high-cycle fatigue behavior for inherently defective butt joints using strain energy density method. International Journal of Fatigue, 193. DOI: https://doi.org/10.1016/j.ijfatigue.2024.108770
[8] Morettini, G., Razavi, S. M. J., Staffa, A., Palmieri, M., Berto, F., Cianetti, F. and Braccesi, C. (2023). On the combined use of averaged strain energy density criteria (ASED) and equivalent material concept (ECC) for the fracture load prediction of additively manufactured PLA v-notched specimens. Procedia Structural Integrity, 47, pp. 296–309. DOI: https://doi.org/10.1016/j.prostr.2023.07.095
[9] Karakaş Ö. (2013). Consideration of mean-stress effects on fatigue life of welded magnesium joints by the application of the Smith–Watson–Topper and reference radius concepts. Int J Fatigue, 49, pp. 1–17. DOI: https://doi.org/10.1016/j.ijfatigue.2012.11.007
[10] Karakaş, Ö., Leitner, M. and Tüzün, N. (2022). Application of critical distance approach for fatigue assessment of welded and HFMI-treated steel joints. International Journal of Fatigue, 154. DOI: https://doi.org/10.1016/j.ijfatigue.2021.106534
[11] Morettini, G., Landi, L., Burattini, L., Stornelli, G., Foffi, G., di Schino, A., Cianetti, F. and Braccesi, C. (2024). Application of the Theory of Critical Distance (TCD) to the Breakage of Cardboard Cutting Blades in Al7075 Alloy. Metals, 14(3). DOI: https://doi.org/10.3390/met14030301
[12] Pelizzari, J., Campagnolo, A., Dengo, C. and Meneghetti, G. (2024). Fatigue lifetime assessment of weld ends with idealized or real geometry in steel joints for off-road vehicles using the Peak Stress Method. International Journal of Fatigue, 178. DOI: https://doi.org/10.1016/j.ijfatigue.2023.107964
[13] Meneghetti, G. and Campagnolo, A. (2020). State-of-the-art review of peak stress method for fatigue strength assessment of welded joints. International Journal of Fatigue, 139. DOI: https://doi.org/10.1016/j.ijfatigue.2020.105705
[14] Chiocca, A. and Frendo, F. (2024). Fatigue assessment of structural components through the Effective Critical Plane factor. International Journal of Fatigue, 189. DOI: https://doi.org/10.1016/j.ijfatigue.2024.108565
[15] Foti, P., Berto, F. and Filippi, S. (2018). Fatigue assessment of welded joints by means of the Strain Energy Density method: Numerical predictions and comparison with Eurocode 3. Frattura ed Integrità Strutturale, 13(47), pp. 104–125. DOI: https://doi.org/10.3221/IGF-ESIS.47.09
[16] Crupi, G., Crupi, G., Crupi, V., Crupi, V., Guglielmino, E. and Taylor, D. (2005). Fatigue assessment of welded joints using critical distance and other methods. Engineering Failure Analysis, 12(1), pp. 129–142. DOI: https://doi.org/10.1016/J.ENGFAILANAL.2004.03.005
[17] Erny, C., Thevenet, D., Cognard, J.-Y. and Körner, M. (2010). Experimental and Numerical Analyses of Fatigue Behavior of Welded Cruciform Joints. Journal of ASTM International, 7(4), pp. 1–15. DOI: https://doi.org/10.1520/JAI102535
[18] Chang, P.-H. and Teng, T.-L. (2008). Numerical and experimental investigation on the fatigue life evaluation of butt-welded joints. Metals and Materials International, 14(3), pp. 361–372. DOI: https://doi.org/10.3365/MET.MAT.2008.06.361
[19] Zou, L., Yang, X., Tan, J., Xu, H. and Sun, Y. (2018). Fatigue life prediction of 5083 and 5A06 aluminum alloy T-welded joints based on the fatigue characteristics domain. Fracture and Structural Integrity, 12(45), pp. 53–66. DOI: https://doi.org/10.3221/IGF-ESIS.45.05
[20] Baumgartner, J., Hobbacher, A. F. and Rennert, R. (2020). Fatigue assessment of welded thin sheets with the notch stress approach – Proposal for recommendations. International Journal of Fatigue, 140. DOI: https://doi.org/10.1016/j.ijfatigue.2020.105844
[21] Pinho de Castro, J. T. and Meggiolaro, M. A. (2013). Is notch sensitivity a stress analysis problem. Fracture and Structural Integrity. 25, pp. 79-86. DOI: https://doi.org/10.3221/IGF-ESIS.25.12
[22] Lazzarin, P. and Tovo, R. (1998). A notch intensity factor approach to the stress analysis of welds. Fatigue & Fracture of Engineering Materials & Structures. DOI: https://doi.org/10.1046/J.1460-2695.1998.00097.X

[23] Pettersson, G. (2002). Fatigue Analysis of a Welded Component Based on Different Methods. Welding in The World, 46(9), pp. 41–51. DOI: https://doi.org/10.1007/BF03377348
[24] Dong, P., Hong, J. K., Osage, D. and Prager, M. (2003). Assessment of ASME's FSRF rules for vessel and piping welds using a new structural stress method. Welding in the World, 47, pp. 31-43. Pressure Vessel Research Council (USA)
[25] Lucertini, S., Morettini, G. and Cianetti, F. (2025). Development of a Numerical Prediction Method for the Strain Energy Density of Welded Joints Using Structural Stresses Derived from Nodal Forces. Engineering Proceedings, 85(1), 32. DOI: https://doi.org/10.3390/engproc2025085032